

Time- and angle-resolved x-ray diffraction to probe structural and chemical evolution during Al-Ni intermetallic reactions

Choong-Shik Yoo, Haoyan Wei, Jing-Yin Chen, Guoyin Shen, Paul Chow et al.

Citation: *Rev. Sci. Instrum.* **82**, 113901 (2011); doi: 10.1063/1.3658817

View online: <http://dx.doi.org/10.1063/1.3658817>

View Table of Contents: <http://rsi.aip.org/resource/1/RSINAK/v82/i11>

Published by the [American Institute of Physics](#).

Related Articles

Interface sharpening in miscible Ni/Cu multilayers studied by atom probe tomography
Appl. Phys. Lett. **99**, 181902 (2011)

Orientation dependence of thermal conductivity in copper-graphene composites
J. Appl. Phys. **110**, 074901 (2011)

An optical magnetic metamaterial working at multiple frequencies simultaneously
Appl. Phys. Lett. **99**, 041109 (2011)

Modulation periodicity dependent structure, stress, and hardness in NbN/W₂N nanostructured multilayer films
J. Appl. Phys. **109**, 123525 (2011)

High-resolution x-ray diffraction investigation of relaxation and dislocations in SiGe layers grown on (001), (011), and (111) Si substrates
J. Appl. Phys. **109**, 123714 (2011)

Additional information on *Rev. Sci. Instrum.*

Journal Homepage: <http://rsi.aip.org>

Journal Information: http://rsi.aip.org/about/about_the_journal

Top downloads: http://rsi.aip.org/features/most_downloaded

Information for Authors: <http://rsi.aip.org/authors>

ADVERTISEMENT

**AIP**Advances

Submit Now

**Explore AIP's new
open-access journal**

- **Article-level metrics
now available**
- **Join the conversation!
Rate & comment on articles**

Time- and angle-resolved x-ray diffraction to probe structural and chemical evolution during Al-Ni intermetallic reactions

Choong-Shik Yoo,^{1,a)} Haoyan Wei,¹ Jing-Yin Chen,¹ Guoyin Shen,²
Paul Chow,² and Yuming Xiao²

¹Department of Chemistry, Institute for Shock Physics, Washington State University, Pullman,
Washington 99164, USA

²HPCAT at Advanced Photon Source, Geophysical Laboratory, Carnegie Institution of Washington,
Argonne, Illinois 60439, USA

(Received 10 May 2011; accepted 16 October 2011; published online 8 November 2011)

We present novel time- and angle-resolved x-ray diffraction (TARXD) capable of probing structural and chemical evolutions during rapidly propagating exothermic intermetallic reactions between Ni-Al multilayers. The system utilizes monochromatic synchrotron x-rays and a two-dimensional (2D) pixel array x-ray detector in combination of a fast-rotating diffraction beam chopper, providing a time (in azimuth) and angle (in distance) resolved x-ray diffraction image continuously recorded at a time resolution of $\sim 30 \mu\text{s}$ over a time period of 3 ms. Multiple frames of the TARXD images can also be obtained with time resolutions between 30 and 300 μs over three to several hundreds of milliseconds. The present method is coupled with a high-speed camera and a six-channel optical pyrometer to determine the reaction characteristics including the propagation speed of 7.6 m/s, adiabatic heating rate of $4.0 \times 10^6 \text{ K/s}$, and conductive cooling rate of $4.5 \times 10^4 \text{ K/s}$. These time-dependent structural and temperature data provide evidences for the rapid formation of intermetallic NiAl alloy within 45 μs , thermal expansion coefficient of $1.1 \times 10^{-6} \text{ K}$ for NiAl, and crystallization of V and Ag_3In in later time. © 2011 American Institute of Physics. [doi:10.1063/1.3658817]

INTRODUCTION

Understanding the dynamic response of solids under extreme conditions of pressure, temperature, and strain rate is a fundamental scientific quest and a basic research need in materials science.¹ Specifically, obtaining an atomistic description of structural and chemical changes of solids under rapid heating and/or compression over a large temporal, spatial, and energy range is challenging but critical to understanding material stability or metastable structure, chemical mechanism, transition dynamics, and mechanical deformation. In this regard, developing time-resolved x-ray diffraction applied to single-event dynamic experiments is timely and synergistic to many proposed activities centered at third- and fourth-generation light sources.²

The high brightness of third-generation (3G) synchrotron x-rays has revolutionized the field of physical sciences, materials research, and bio- and geo-sciences in recent years. The machine characteristics of 3G synchrotrons are ideally suitable for probing dynamic phenomena with a fast time-resolution even in ps. Yet, these measurements are mostly concentrated on probing non-single event phenomena where the signal can be averaged over multiple x-ray exposures. Because of an insufficient amount of x-ray photons, the application of time-resolved x-ray diffraction to single event phenomena is largely limited to single crystals with known structures.³ Obtaining a powder x-ray diffraction with a reasonable signal to noise ratio requires an order of 10^6 – 10^7 photons, which translates into roughly 10–100 bunches of x-ray

pulses ($\sim 10^5$ photons per bunch at 16IDD station/Advanced Photon Source (APS), for example) from a typical 3G synchrotron source. Hence, in order to obtain time-resolved structural information of polycrystalline samples, it is necessary to accumulate the x-rays over an order of μs even using x-rays from an undulator at 3G synchrotron sources. On the other hand, the 4G light source such as the linac coherent light source can provide substantially brighter x-rays in sub ps,⁴ but it too is limited to obtaining a structural snap shot rather than a structural evolution during the phase and chemical changes which occur over a long time period of interest.

Because of high spatial resolution and high brilliance, synchrotron x-rays have been widely utilized to develop time-resolved x-ray diffraction techniques. Previous efforts on *in situ* structural characterization of single event phenomena have achieved a time resolution of only about milliseconds limited by slow detectors.⁵ Recently, two research groups have accomplished a substantially faster time resolution to 50 μs and 125 μs using 2D and 1D pixel detectors, respectively, in studies of Al-Ni intermetallic reactions.^{6–8} These methods, however, have several limitations: (1) a limited range of reciprocal space between 2 and 4 \AA^{-1} ,^{6,7} which makes it difficult to solve unknown structures; (2) a discrete recording of detector with a down time of 5 μs to 125 μs between each exposure for data readout;⁸ (3) to reduce the amount of data that can be handled, the pixel array detector has a small active area ($15 \times 13.8 \text{ mm}^2$, 100×92 pixels) and can only record a small (eight) number of successive frames; and⁶ (4) for the angular detector, 1D diffraction lines instead of 2D diffraction rings are recorded.⁸

In this paper, we report a simple yet powerful time- and angle-resolved x-ray diffraction (TARXD) technique based on

^{a)} Author to whom correspondence should be addressed. Electronic mail: csyoo@wsu.edu. Tel.: (509) 335-2712.

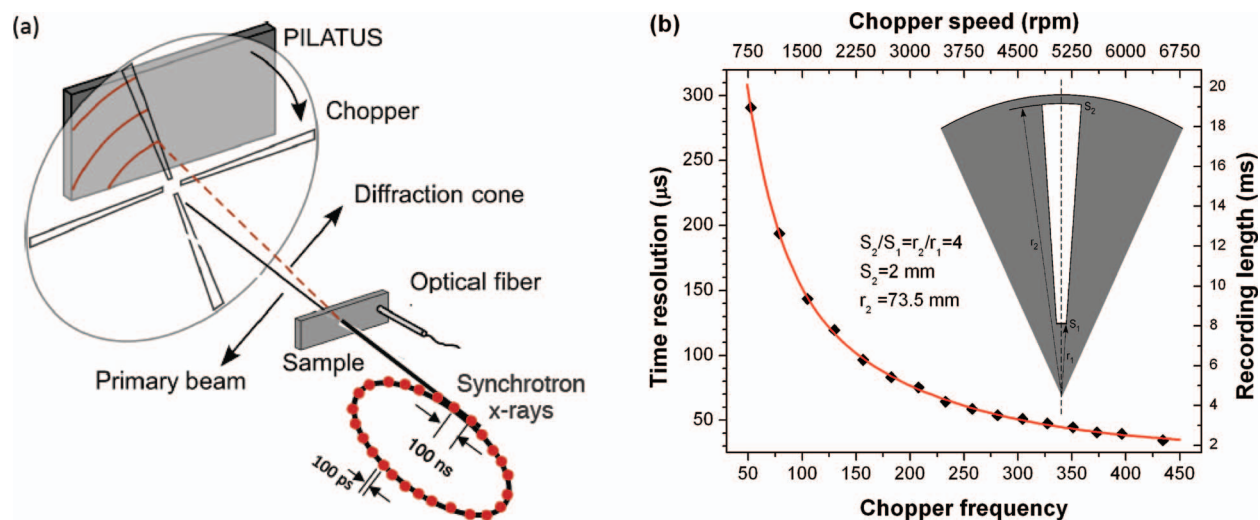


FIG. 1. (Color online) (a) A schematic of TARXD setup to probe structural and chemical evolutions during rapidly propagating intermetallic reactions. The system employs intense monochromatic synchrotron x-rays, a 2D array detector (PILATUS) and a custom-designed diffraction chopper. (b) Plots of time-resolution (or x-ray exposure time) and recording time in each 2D detector frame as a function of chopper frequency (or rotation speed). The inset shows the slot opening of chopper (1.56°), which defines the x-ray exposure time.

a custom-designed fast-rotating diffraction beam chopper and a large 2D pixel array x-ray detector (PILATUS 100 K). The chopper resolves the powder diffraction beam, *spatially*, into a time domain with a resolution in microseconds, which is then recorded onto a large 2D pixel array detector, *continuously*, over a long time period (several milliseconds). Hence, the present method eliminates the need for expensive and sometimes difficult-to-find fast detectors and overcomes the most of above-mentioned limitations.

EXPERIMENTS

Time-resolved synchrotron x-ray diffractions for single event phenomena are typically obtained using an x-ray streak camera and an intensified 2D-charge coupled device (CCD)³ or a fast 1D pixel array detector.²⁻⁴ The former is limited by low sensitivity of a phosphor screen in the x-ray streak camera and high noise in an intensified CCD, yet the latter by a relatively long read-out time ($\sim 100 \mu\text{s}$) of an array detector, a relatively small readout capability, and a low signal collection. Therefore, our approach is to use a 2D pixel array detector (PILATUS) in combination with a fast running chopper (Fig. 1). The PILATUS detector is a silicon hybrid pixel detector system with a high dynamic range over five orders, high count rate capability in $> 2 \times 10^6$ photons/s/pixel, high detection efficiency of nearly single photon counting (99% at 8 keV and 55% at 15 keV), and a very good point spread function. It has been developed to achieve the best possible signal to noise ratio for a protein crystallography at the Paul Scherrer Institute.^{9,10} It has nearly a same level of sensitivity as an intensified x-ray CCD but a substantially reduced noise level. However, because of its long read out time of a large number of 2D pixels (~ 2.7 ms for PILATUS 100 K), it is typically used for static powder x-ray diffractions or time-resolved x-ray diffraction in a gated mode in a pump-probe experiment.¹¹

To overcome this limitation, we use a fast-rotating diffraction beam chopper made of a metal disc (150 mm in diameter), which has four orthogonal opening slots of 1.56° . In this configuration, a quarter turn of the chopper covers the entire detector area of $83.8 \times 33.5 \text{ mm}^2$ with 487×195 pixels (pixel size $172 \times 172 \mu\text{m}^2$). The diffraction chopper is placed in front of the detector, and the incident beam is aligned to the center of the disc as close as possible. As the disc rotates, the slot will sweep across the entire detector active area, clockwise, along the Debye-Scherrer's rings. Thus, only small portions of diffraction rings are recorded at different azimuth angles of the detector at different times. In the present setup, it is noteworthy that unlike the previous time-resolved method utilizing in-line chopper for the primary x-ray beam,¹² the diffraction beam is dispersed as a function of time to record the materials structural change. As the diffraction arcs are recorded continuously, there is no down time between different time stamps within the first frame of the detector, which is critical to capture the entire picture of the rapidly propagating reaction. At the maximum rotation speed of the chopper ~ 6750 rpm, the system yields a time-resolution of $\sim 35 \mu\text{s}$ and a total continuous recording time of 2.3 ms on each frame (Fig. 1(b)). The time-resolution is defined as the full-opening time as the slot passes in front of a pixel. Operating the detector in a kinetic mode, multiple frames can be recorded over several hundreds of milliseconds with a relatively small read out time of 2.7 ms between the frames.

To demonstrate the capability of the present TARXD technique, we use Al-Ni nanofoils from Reactive Nano Technologies Inc. The foil samples are made of 24 nm Al and 16 nm Ni multilayers with an overall thickness of $40 \mu\text{m}$, which translates to an atomic ratio of about 1:1. The Ni layers contain 10 at.% V that is added to render a non-magnetic sputtering target.¹³ The nanofoil surfaces are also coated with a very thin INCUSIL solder layer ($1 \mu\text{m}$ or less) containing Ag, Cu, and In.¹⁴ The presence of V and INCUSIL solder are

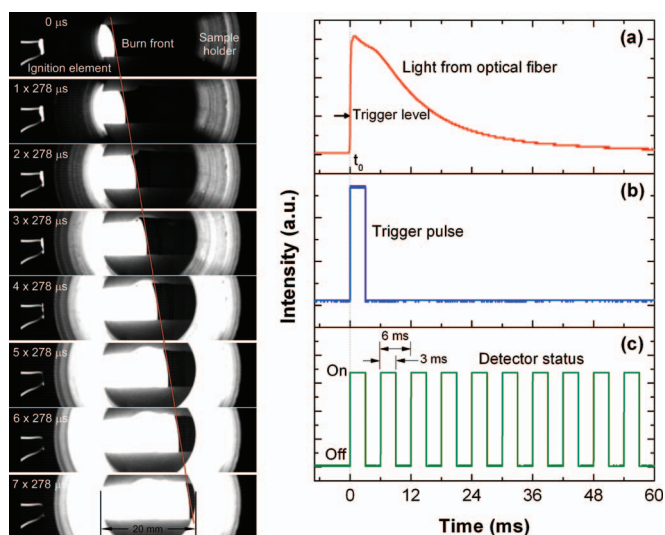


FIG. 2. (Color online) (Left panel) A series of micro photographic images showing highly exothermic intermetallic reactions between Ni and Al nano-multilayers. The burn front speed gives the reaction propagation rate of 7.7 m/s. (Right panel) The optical signal measured by an optical fiber (a), which is used to generate a triggering signal (b) for the PILATUS detector as shown in (c) for a high time-resolution mode. Note that the detector is “off” for ~ 3 ms between the frames (“On”) to read and store the data.

not expected to interfere with the Al-Ni chemical reaction, but provide a good test for the sensitivity of the present TARXD system in probing such minor impurities, as will be shown later.

Upon heating, the nanofoil samples undergo highly exothermic intermetallic reactions between Al and Ni on a time-scale of microseconds—ideal to test the current TARXD system. Figure 2 (left panel) illustrates a series of high-speed camera images showing the propagation of reaction front. These images were originally recorded at 54 000 frames per second, but only those frames selected every 278 μ s are shown in the figure. The sample strip was sandwiched between two ring holders. On the left, a Nichrome wire was utilized as an ignition element to thermally start the reaction. The red lines indicate the position of the reaction front. Based on this slope, we obtain the propagation speed of 7.6 m/s, reproducible over a large number of measurements and also consistent with the previously estimation of 7.3 m/s.⁸ Thus, we used this signal for precise timing of the present time-resolved experiments, as illustrated in Fig. 2 (right panel).

As shown in Fig. 2(a) (right panel), the emitted light from the Al-Ni chemical reaction was measured by a photodiode (PD) through a 1-mm diameter optical fiber at ~ 6 mm away from the x-ray beam center. The PD is obtained from Thorlabs (Model DET10A, 10 V bias voltage). The PD output was then directly fed into a digital delay generator (Berkeley Nucleonics 505) to produce an electrical pulse of 3 ms duration at a designated trigger level (Fig. 2(b)). The sharp leading edge of this electrical pulse (around nanoseconds) was used to trigger the x-ray detector and any other recording devices such as an oscilloscope. The detector worked in a kinetic mode, recording successive exposures of 3 ms with same readout time in between, as shown in the feedback signal of the detector in Fig. 2(c)(right panel).

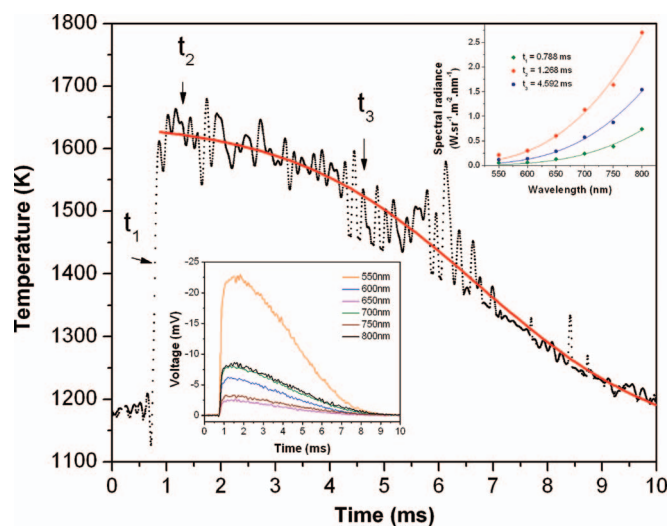


FIG. 3. (Color online) Time-resolved temperature changes during the initial stage of intermetallic reactions between Ni and Al nano-multilayers showing together with the raw PMT records of six optical channels set at different wavelengths in the lower inset and the gray body fits of the records at times noted as t_1 , t_2 , and t_3 in the upper inset. The time zero signifies the instant of trigger and the reaction starts with an induction period of ~ 700 μ s and reaches the peak temperature of 1680 K within ~ 100 μ s then cools down over the next 10 ms.

The temperature evolution during the reaction was measured by using an optical pyrometer following the Planck’s law. The pyrometer has six measurement channels constructed using Hamamatsu H7732P-11 photomultiplier tubes (PMTs) with a rise time of 2.2 ns. A narrow bandpass filter ($\Delta\lambda = 10$ nm at FWHM) was placed in front of each PMT to define the wavelength in the range between 550 nm and 800 nm every 50 nm increments. Neutral density filters were also placed in front of each PMT to regulate the incident light intensity within the linear response regime. The incident light was transmitted through 200 μ m diameter optical fibers to each PMT. On the pyrometer probe side, they were arranged in a hexagonal pattern forming a 7-in-1-fiber bundle. The extra one (center fiber) was used for alignment. After PMTs, two Tektronix digital phosphor oscilloscopes (DPO2000 series of bandwidth 100–200 MHz) were used to record and display the signals from PMTs. Terminators of 50 Ω impedance were connected in parallel with the oscilloscopes to match the cable impedance in order to avoid signal distortion from reflections. Before measurements, the entire pyrometer system, including PMTs, fibers, filters, and other optics used, was calibrated with a blackbody radiation source from Optronic Laboratories (OL 480).

Time-resolved temperatures of the sample (Fig. 3) are obtained by fitting the measured emission intensities at six discrete wavelengths between 550 nm and 800 nm to a grey body radiation equation (see the insets). On the leading edge, the temperature rises from 1200 K to 1600 K in about 100 μ s, consistent with the phase transformation window observed from the x-ray diffraction data (Fig. 4). Accordingly, the reaction heating-rate of the present 40 μ m-foil is $\sim 4 \times 10^6$ K/s—fast enough to be considered as an adiabatic heating. In fact, the measured peak temperature 1680 (± 100) K is nearly same (within the uncertainty) as the previously measured 1740 K

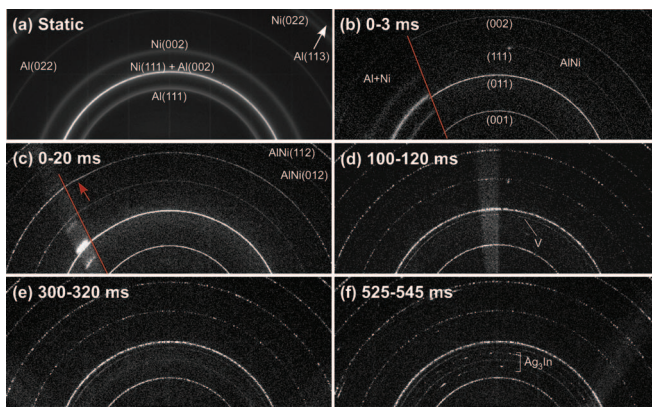


FIG. 4. (Color online) TARXD of Ni-Al nano-multilayers in static (a) and dynamic (b-f) conditions probing the intermetallic reaction yielding AlNi alloy. The record (b) was obtained in high time-resolution of $45 \mu\text{s}$, whereas those of (c-f) were in low time-resolution of $280 \mu\text{s}$. The red lines in (b) and (c) signify the onset of the reaction. The diffraction lines of Al, Ni, and AlNi are indexed for comparison. Note that broad diffraction lines of unreacted Al and Ni nano-layers and sharp lines of AlNi products which develop larger crystallites over ~ 10 ms (c). Also, note that on a set of new diffraction lines from V and Ag_3In appears in (d) and (f).

for the $30 \mu\text{m}$ -foil,⁷ and slightly lower than the calculated value 1840 K based on an adiabatic approximation.^{7,15} After the temperature reaches the peak value, it gradually decreases in a sigmoidal mode for the next 10 ms, yielding

an average cooling rate of about $4.8 \times 10^4 \text{ K/s}$ —100 times slower than the heating rate. Note that the peak temperature is much higher than the melting temperature of Al (933 K at ambient pressure) but lower than those of Ni (1726 K) and AlNi (1911 K). Because of the limited spectral range below 800 nm and relatively low thermal emission intensity, the present pyrometer is only suitable for temperatures higher than 1200 K.

RESULTS AND DISCUSSION

All diffraction experiments were carried out using monochromatic synchrotron x-rays at 14.353 keV (or 0.8638 \AA in wavelength) from an undulator at the 16IDD station of the Advanced Photon Source. The x-ray beam size is focused down to $\sim 100 \mu\text{m}$ with Kirkpatrick-Baez mirrors. Figure 4 shows (a) angle-resolved x-ray diffraction (ARXD) of the Ni-Al sample in a static condition and (b) TARXD of the sample during the first 3 ms of the reaction recorded with an exposure time of $\sim 45 \mu\text{s}$. Figures 4(c)–4(f) show another set of diffraction images recorded at substantially low time-resolution: a $280 \mu\text{s}$ exposure time and a 20 ms frame time with a 3 ms black-out time between the frames. Nevertheless, the initial chemical reaction can still be clearly observed in the first exposure (Fig. 4(c)). Time runs clockwise, and the onset of reaction is marked in red lines in Figs. 4(b) and 4(c). A

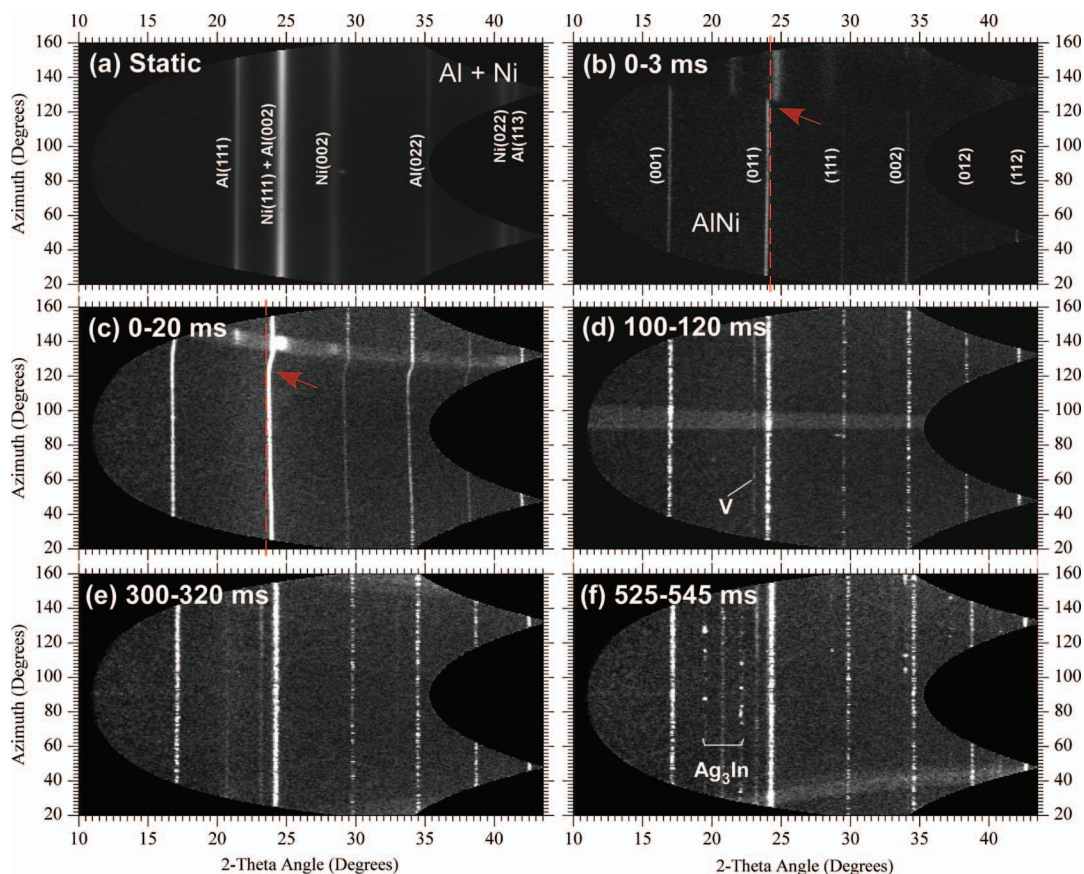


FIG. 5. (Color online) Caked images of TARXD images in Fig. 4, as plotted in the 2θ (Bragg angles) vs. azimuth angles (time). The vertical lines in (b) and (c) signify thermal expansion of the AlNi (110) lattice during the initial reaction period and thermal contraction during the later cooling period. This thermal cycle effects result in kinks in the diffraction lines as indicated by a red arrow in (c). The onset of the reaction is also marked by an arrow in (b). The diffraction lines for Al, Ni, and AlNi are indexed in (a) and (b) and those from V and Ag_3In are marked in (d) and (f), as shown in Fig. 4.

small segment of white strip in Fig. 4(c) is the region where double exposure occurs because of the overlap of the signal from the next incoming slot.

Several features are pertinent to these TARXD records: (1) the broad Debye-Scherrer's diffraction rings from unreacted Al and Ni nano-layers. Based on the Scherrer equation, it gives the grain size of 12 nm for Al and 7 nm for Ni—about the half the layer thickness. (2) Relatively sharp diffraction rings from the product of AlNi, which appear initially continuous but later become spotty, indicating development of large grain products over roughly 10 ms time period. (3) Some additional features appear in later times of about 100 ms (d) and 500 ms after the initial reaction (f). These features, respectively, correspond to the diffraction features of V (*bcc*, *Im-3m*) and Ag_3In (*hcp*, $P6_3/mmc$) as previously observed.⁸

Figure 5 plots the “caked” records of angle-resolved diffraction images in Fig. 4 in the Bragg angle (or 2θ) vs. the azimuth angle (or time). Similarly, the onset of the reaction is marked by a red arrow in Fig. 5(b), and the diffraction lines are also indexed. By integrating the caked diffraction patterns for an arbitrary time period (Δt), we then obtain time-resolved diffraction patterns as shown in Fig. 6. The static pattern clearly represents that of Al and Ni nanolayers in *fcc* with the lattice parameters of 4.031 Å and 3.518 Å, respectively. These measured lattice parameters are slightly smaller than the bulk values of Al (4.040 Å) and Ni (3.524 Å). As the reaction propagates to the X-ray probing site (at ~ 770 μs after the ignition), a new set of sharp diffraction lines (at ~ 17 , 24 and 35 degrees) appears indicating the onset of reaction. These features can be easily assigned to a cubic (*Pm-3m*) structure of AlNi with the lattice parameter of $a = 2.893$ Å—about 0.45% larger than that at ambient condition 2.880 Å.¹⁶ This initial reaction occurs within 45 μs , evident from the coexistence of the reactants and product only at 767–812 μs . At substantially later times (100–500 ms after the initial reactions), there are several diffraction features from minor impurities of V at around 100–120 ms and Ag_3In at ~ 200 ms and after. The measured lattice parameters of $a = 3.026$ Å for *bcc* V and $a = 2.927$ Å and $c = 4.765$ Å for *hcp* Ag_3In are in good agreement with those reported; $a = 3.030$ Å for V and $a = 2.956$ Å and $c = 4.786$ Å for Ag_3In .^{17,18} The observation of these by-products, on the other hand, demonstrates the capability of the present TARXD, using a large 2D pixel array detector in combination with a fast running chopper, to probe structural and chemical changes over a long period time with relatively high time and spatial resolutions.

The present TARXD provides a high-resolution image over a wide range of Bragg angles (2θ to 45°), sufficient to characterize unknown crystal structures across the phase and chemical changes as well as to determine thermoelastic properties accurately. For example, note on the subtle shift of the (011) diffraction line of AlNi (marked by the red vertical lines in both Figs. 5(b), 5(c), and 6). The lattice expansion and retraction lead to the kinks in the diffraction lines as indicated by the red arrows in Figs. 4(c) and 5(c). This clearly indicates that the lattice expands during the initial stage of reaction (to 4–7 ms), then slowly returns back to the ambient value ($a = 2.893$ Å) in later times over nearly 5 s, as illustrated in Fig. 7. Based on these results, we estimate a linear thermal ex-

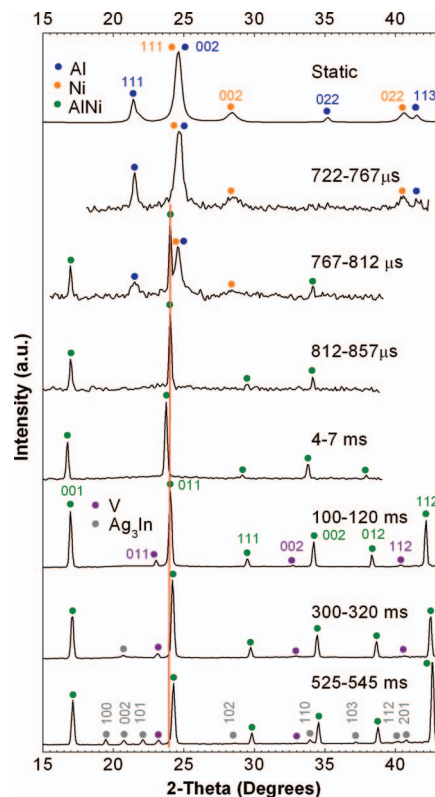


FIG. 6. (Color online) ARXD patterns of reacting Ni-Al multilayers at discrete times obtained by integration of the caked images over a discrete time period. Also marked are the (hkl) indexes of different chemical species. The shift of the diffraction lines as indicated by the red lines indicates the lattice expansion and contraction of AlNi compound formed in the reaction.

pansion coefficient of 1.1×10^{-6} K for NiAl—in good agreement with the previously calculated value 1.4×10^{-6} K¹⁹ and the measured ones, 1.2×10^{-6} K²⁰ and 1.5×10^{-6} K.⁸ The data in Fig. 7 also yield the thermal conduction rate of 4.5×10^4 K/s for NiAl.

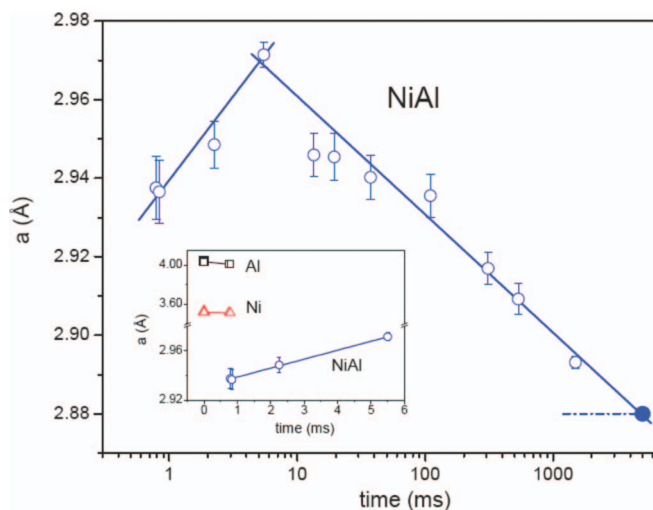


FIG. 7. (Color online) The lattice parameters of Al, Ni, and AlNi (open symbols) plotted as a function of time. It shows the lattice changes during the exothermic intermetallic reaction and subsequent cooling. The lattice parameters at ambient conditions are also marked in solid symbols for comparison.

CONCLUSIONS

We have presented TARXD capable of probing structural and chemical evolutions during the intermetallic reactions of nano-multilayer between Al and Ni in a microsecond time resolution over a long time (nearly a second) of interest. The TARXD data show rapid formation of NiAl intermetallic phase and later-time crystallization of V and Ag₃In, as well as determine a linear thermal expansion coefficient of 1.1×10^{-6} K for NiAl.

The present method employs a high-resolution 2D PILATUS detector in combination with a fast running diffraction chopper, offering a new way of obtaining time-resolved powder x-ray diffraction patterns in a microsecond time resolution with high sensitivity nearly comparable to an intensified CCD but a substantially lower level of noise. The simplicity of the present TARXD method is also beneficial, as it can be readily applicable to a wide range of dynamic experiments to study both single event phenomena of solids under thermal, electric, or mechanical impact conditions and non-single event changes using dynamic-DAC and high frequency pulse lasers. The time resolution of the system can be enhanced to 1 μ s or better simply by use of a faster chopper and a narrower slot, as long as there are sufficient x-ray photons for powder diffraction. The spatial-resolution can also be increased by use of a larger detector such as PILATUS 300 K or 2 M of which active area can be 10–100 times of the present one. Operating synchronously with an in-line x-ray chopper, it may be even feasible to perform a single-bunch (100 ps) time-resolved powder x-ray diffraction of single dynamic events on the proposed Energy Recovery Linac (ERL).²¹

ACKNOWLEDGMENTS

The x-ray work was done using the HPCAT beamline (16IDD station) of the APS. The present study has been supported by the U.S. DHS under Award No. 2008-ST-061-ED0001 and NSF-DMR (Grant No. 0854618). The views and conclusions contained in this paper are those of the authors and should not be interpreted as necessarily representing the official policies, either expressed or implied, of the U.S. Department of Homeland Security.

- ¹See http://www.er.doe.gov/bes/reports/files/MUEE_rpt.pdf for a DOE-BES report on Basic Materials Needs for Materials under Extreme Environments.
- ²Y. M. Gupta and C. S. Yoo, *Dynamic Compression Collaborating Access Team (DC-CAT) at Advanced Photon Source*, a Letter of Intent submitted to the APS (2008); A. Goncharov, *Time Resolved X-ray Diffraction and Spectroscopy under Extreme Conditions*, a proposal proposed to NSLS-II (2010); R. Hemley, N. Ashcroft, R. Hoffman, and J. Paraise, *High Pressure Science at the Edge of Feasibility*, June 23–24, 2011, Cornell, New York, also see <http://www.lepp.cornell.edu/Research/AP/ERL/> for the development of the Energy Recovery Linac; H. J. Lee, B. Nagler, J. Hastings, and R. W. Lee, *Matter in Extreme Conditions Instrument with LCLS for the Study of High Energy Density Physics*, 2010 APS, November 8–12, 2010, Abs#PO6.001.
- ³S. J. Turneaure, Y. M. Gupta, K. Zimmerman, K. Perkins, C. S. Yoo, and G. Shen, *J. Appl. Phys.* **105**, 053520 (2009).
- ⁴H. N. Chapman *et al.*, *Nature* **470**, 73 (2011).
- ⁵F. Bernard, E. Gaffet, M. Gramond, M. Gailhanou, and J. C. Gachon, *J. Synchrotron Radiat.* **7**, 27 (2000).
- ⁶J. C. Trenkle, L. J. Koerner, M. W. Tate, S. M. Gruner, T. P. Weihs, and T. C. Hufnagel, *Appl. Phys. Lett.* **93**, 081903 (2008).
- ⁷J. C. Trenkle, L. J. Koerner, M. W. Tate, N. Walker, S. M. Gruner, T. P. Weihs, and T. C. Hufnagel, *J. Appl. Phys.* **107**, 113511 (2010).
- ⁸K. Fadenberger, I. E. Gunduz, C. Tsotsos, M. Kokonou, S. Gravani, S. Brandstetter, A. Bergamaschi, B. Schmitt, P. H. Mayrhofer, C. C. Doumanidis, and C. Rebholz, *Appl. Phys. Lett.* **97**, 144101 (2010).
- ⁹P. Kraft, A. Bergamaschi, Ch. Brönnimann, R. Dinapoli, E. F. Eikenberry, H. Graafsma, B. Henrich, I. Johnson, M. Kobas, A. Mozzanica, C. M. Schepütz, and B. Schmitt, *IEEE Trans. Nucl. Sci.* **56**, 758 (2009).
- ¹⁰C. Brönnimann, S. Florin, M. Linder, B. Schmitt, and C. Schulze-Briesse, *J. Synchrotron Radiat.* **7**, 301 (2000).
- ¹¹T. Ejdrup, H. T. Lemke, K. Haldrup, T. N. Nielsen, D. A. Arms, D. A. Walko, A. Miceli, E. C. Landahl, E. M. Dufresne, and M. M. Nielsen, *J. Synchrotron Radiat.* **16**, 387 (2009).
- ¹²A. McPherson, J. Wang, P. L. Lee, and D. M. Mills, *J. Synchrotron Radiat.* **7**, 1 (2000).
- ¹³M. P. Blickley, N. A. Soroka, J. D. Demaree, J. K. Hirvonen, and P. G. Dehmer, *MRS Proc.* **908**, 0908001426 (2005).
- ¹⁴See www.morgantechnicalceramics.com for the data sheet for INCUSIL. Silver/copper based brazing alloy with the composition of 59.0% Ag, 27.25% Cu, 12.50% In and 1.25% Ti.
- ¹⁵A. J. Gavens, D. Van Heerden, A. B. Mann, M. E. Reiss, and T. P. Weihs, *J. Appl. Phys.* **87**, 1255 (2000).
- ¹⁶H. E. Swanson, H. F. McMurdie, M. C. Morris, and E. H. Evns, *Natl. Bur. Stand. Monogr.* **25**, 82 (1968).
- ¹⁷R. W. G. Wychoff, *Crystal Structures* (Wiley, New York, 1963), Vol. 1, p. 16.
- ¹⁸D. P. Morris and L. Williams, *Acta Crystallogr.* **14**, 74 (1961).
- ¹⁹Y. Wang, Z.-K. Liu, and L.-Q. Chen, *Acta Mater.* **52**, 2665 (2004).
- ²⁰Y. S. Touloukian, R. K. Kirby, R. E. Taylor, and P. D. Desai, *Thermophysical Properties of Matter Thermal Expansion* (Plenum, New York, 1975).
- ²¹D. H. Bilderback, P. Elleaume, and E. Weckert, *J. Phys. B* **38**, S773 (2005).